ANTIBACTERIAL ACTIVITY OF g-C_3N_4/$ZnWO_4$ NANORODS

AYYAPPAN S[1*] & NITHYA R[2]

[1*]Associate Professor, Government College of Engineering, Salem, Tamil Nadu, India
[2] Research Scholar, Government College of Engineering, Salem, Tamil Nadu, India

Keywords: *g-C_3N_4/$ZnWO_4$, Escherichia coli, Staphylococcus aureus and Cytotoxicity*

ABSTRACT

In this study, we synthesized g-C_3N_4/$ZnWO_4$ nanorods and evaluated their antibacterial activity against *Escherichia coli* and *Staphylococcus aureus*. Additionally, we assessed the cytotoxicity of these nanorods to determine their safety for potential applications. The g-C_3N_4/$ZnWO_4$ nanocomposite demonstrated a significant zone of inhibition (ZOI) against *E. coli* at an optimal concentration of 100 µg/disk. This strong inhibition can be attributed to the physicochemical interactions between the nanocomposite and the bacterial surface.

1. INTRODUCTION

Bimetallic nanoparticles have been synthesized on semiconducting supports to enhance their catalytic efficiency. Materials like graphene and carbon nitride have been successfully utilized as solid supports for the synthesis of metal and metal oxide nanoparticles (NPs) in catalysis and electrocatalysis. Carbon nitride (g-C_3N_4) is a visible-light-active photocatalyst, attributed to its unique electronic band structure and layered configuration. The advantages of g-C_3N_4 as a support for electrocatalytic reactions are numerous. The presence of heteroatoms, such as nitrogen-based ligands and repetitive s-triazine units in the g-C_3N_4 structure, facilitates coordination and stabilization with nanoparticles. This strong interaction between metal NPs and the substrate can enhance electrical connectivity and electron transport. The synthesis of palladium (Pd) and platinum (Pt) NPs on nitrogen-doped mesoporous carbon for electrocatalysis, demonstrating that nitrogen functional groups improve NP-substrate interactions [1]. The developed Pt-Ni and Pt-Fe core-shell carbon nitride nano photocatalysts, highlighting the strong metal-ligand interactions [2]. Nitrogen doping in carbon nanotubes (CNTs) enhances the photocatalytic activity of loaded Pt/CNT catalysts, with nitrogen atoms contributing to increased active sites that improve charge transfer during electrocatalysis [3]. The synthesized cobalt (Co) and carbon-doped g-C_3N_4

 https://doi.org/10.5281/zenodo.13943054

nanosheets, achieving enhanced photocatalytic activity and improved interactions between Co and C due to accessible nitrogen functionalities, which also facilitate better charge transfer [4]. Additionally, the durability of the catalyst on the electrode surface is significantly enhanced in the presence of g-C_3N_4. The decorated Pd NPs on porous carbon nitride surfaces for oxidation and hydrogen evolution. Recently, our group reported the synthesis of monometallic (Au and Pd) and bimetallic (Au-Pd) NPs using g-C_3N_4 quantum dots (QDs) as stabilizing agents for nitrophenol reduction. The synthesis of $ZnWO_4$ bimetallic NPs on graphitic carbon nitride surfaces using hydrazine as a reducing agent, demonstrating higher photocatalytic activity in oxygen reduction and hydrogen evolution reactions [5].

Antimicrobial activity

The availability and use of a wide variety of antibiotics and antimicrobial products have significantly reduced complications related to infectious diseases. However, excessive use of these agents over the years has led to an increase in drug-resistant pathogens. Microbial multidrug resistance poses serious risks, prompting research into alternatives for antimicrobial treatment. Among various strategies, the use of nanostructures is particularly promising due to their high surface-to-volume ratio and the potential for chemically incorporated antibacterial activity. Graphene, a two-dimensional nanomaterial, exhibits excellent biocompatibility, making it suitable for a range of applications, including biosensing, drug delivery, biomedical device development, diagnostics, and therapeutics [6]. Graphene-based nanostructures show great promise in the fight against microbial infections.

In this study, we evaluated the antibacterial activities of our samples against both Gram-negative (*E. coli*) and Gram-positive (*S. aureus*) bacteria, as well as the antifungal activity against *Candida albicans*. The antimicrobial activity of all powder samples was assessed using a modified Kirby-Bauer disk diffusion method. Moderate zones of inhibition were observed for all samples against both *S. aureus* and *E. coli*, as well as against *Candida albicans*.

Gram-negative and Gram-positive bacteria

Bacteria are microscopic single-celled organisms that thrive in diverse environments. They can live within soil, in the ocean and inside the human gut. Human's relationship with bacteria is complex. Sometimes they lend a helping hand, by curdling milk into yogurt or helping with our digestion. At other times they are destructive, causing diseases like pneumonia. In the present work the antibacterial activity of as synthesized nanoparticles against two Gram positive

 https://doi.org/10.5281/zenodo.13943054

(Staphylococcus aureus) and Gram negative (Escherichia coli) bacterial strains were studied. Introduction sets to the stage well for discussing the dual nature of bacteria and the role of nanoparticles in antibacterial research [7]. You might want to elaborate on the specific types of nanoparticles you're studying, their synthesis methods, and the mechanisms by which they exert antibacterial activity. Additionally, providing context on the significance of targeting both Gram-positive and Gram-negative bacteria could enhance your work.

Staphylococcus aureus

Staphylococcus aureus (S.aures) is a gram-positive bacterium found in the nose, respiratory tract and on the skin as shown in fig 1. It can cause a range of illnesses, from minor skin infections to life threatening diseases such as pneumonia, meningitis, osteomyelitis, endocarditis, toxic shock syndrome, bacteraemia and sepsis [8].

Figure 1 Structure of Gram-Positive Bacterial Strain

Escherichia coli

Escherichia coli, also known as E.coli is a gram negative, anaerobic, rod shaped bacterium of the genus Escherichia is commonly found in the lower of warm blooded organisms which causes the majority of urinary tract infections [9] as shown fig 2.

 https://doi.org/10.5281/zenodo.13943054

Figure 1.1 Structure of Gram-Negative Bacterial Strains

2. MATERIALS AND REAGENTS

Thiourea, zinc nitrate [$Zn(NO_3)_2 \cdot 6H_2O$], sodium tungstate [$Na_2WO_4 \cdot 2H_2O$], cetyltrimethylammonium bromide (CTAB), sodium hydroxide (NaOH), sulfuric acid (H_2SO_4), and ethanol were purchased from Merck. All chemicals were of analytical grade and were used as received, without further purification.

Synthesis of g-C_3N_4/$ZnWO_4$ nanoparticles

In this work, a g-C_3N_4 coupled $ZnWO_4$ nanocomposite was prepared using a cost-effective hydrothermal method. The process began by dissolving 0.5 M g-C_3N_4 in 100 mL of deionized water, followed by sonication for approximately 45 minutes to achieve a homogeneous dispersion. To this dispersion, 50 mL of 0.7 M zinc nitrate [$Zn(NO_3)_2 \cdot 6H_2O$] and 0.3 M sodium tungstate [$Na_2WO_4 \cdot 2H_2O$] were added while stirring magnetically. Under continuous stirring, 0.05 M cetyltrimethylammonium bromide (CTAB) was introduced, and the pH of the solution was adjusted to 10 through the dropwise addition of 0.05 M sodium hydroxide (NaOH). After stirring for about 1 hour, the homogeneous mixture was transferred to a Teflon-lined autoclave and maintained at 150°C for 14 hours. Upon completion of the hydrothermal process, the autoclave was allowed to cool to room temperature.

A yellowish-white powder was then obtained, which was washed several times with deionized water and ethanol to remove alkaline residues from the nanoparticle surfaces, and

 https://doi.org/10.5281/zenodo.13943054

subsequently dried in air. This experimental procedure was adapted to prepare three different molar concentrations (3, 5, and 7 mol %) of $ZnWO_4$ on g-C_3N_4.

3. ANTI-BACTERIAL ACTIVITY

It has been demonstrated that carbon-based materials and metal oxide nanoparticles exhibit effective antimicrobial properties against common waterborne pathogens [10].

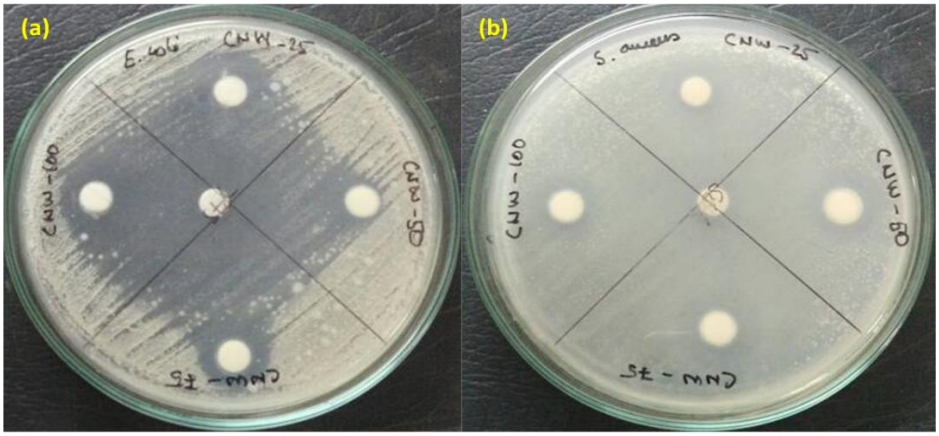

Figure 3 Antibacterial activity against Gram positive and Gram negative bacteria of g-C_3N_4/$ZnWO_4$ nanorods

In this study, we analyzed the antibacterial properties of the as-synthesized g-C_3N_4/$ZnWO_4$ nanocomposite against Gram-positive and Gram-negative clinical pathogens, specifically *E. coli* and *S. aureus*. Our results revealed that the $ZnWO_4$-doped g-C_3N_4 exhibited strong inhibitory activity, with a larger zone of inhibition compared to pristine g-C_3N_4. The g-C_3N_4/$ZnWO_4$ nanocomposite demonstrated a significant zone of inhibition (ZOI) against *E. coli* at an optimal concentration of 100 µg/disk. This strong inhibition can be attributed to the physicochemical interactions between the nanocomposite and the bacterial surface. The fine crystalline structure and incorporation of dopants in the g-C_3N_4/$ZnWO_4$ nanocomposite enhance the transfer of photogenerated electrons and holes between the core and the catalyst surface, which further improves its antimicrobial efficacy. The g-C_3N_4/$ZnWO_4$ nanoparticles primarily target the outer surface (cell wall) of the bacterial strains. The cell wall of bacteria is a complex structure composed of lipopolysaccharides (in Gram-negative bacteria) and peptidoglycan (in Gram-positive bacteria) [11,12]. *E. coli*, having a higher number of anionic groups, interacts electrostatically with the polycationic structure of the g-C_3N_4/$ZnWO_4$ nanocomposite. Notably, the g-C_3N_4/$ZnWO_4$

https://doi.org/10.5281/zenodo.13943054

nanocomposite significantly reduces bacterial growth in *E. coli* compared to *S. aureus*, with a higher zone of inhibition observed for the Gram-positive bacteria as shown fig 3.

Table 1 Antibacterial activity against positive and negative Gram bacterial strain of g-C_3N_4/$ZnWO_4$ nanoparticles

S.No	Bacterial Strain	Zone of Inhibition(mm)				
		Standard ciprofloxacin (10µg/disk)	g-C_3N_4/$ZnWO_4$ nanorods (25 -100µg/disk)			
			25	50	75	100
1.	*Escherichia coli*	52	30	35	41	44
2.	*Staphylococcus aureus*	39	12	15	17	19

4. CYTOTOXICITY EVALUATION OF g-C_3N_4/$ZnWO_4$

The dose-dependent cytotoxicity of the rod-like g-C_3N_4/$ZnWO_4$ nanoparticles was evaluated against the L929 cell line. The percentage of cell viability following continuous incubation for 48 hours at various concentrations is depicted in Fig. [insert figure number]. The L929 cell line was procured from the National Centre for Cell Science (NCCS), Pune, India. Cultured cancer cells are valuable for the rapid screening of potential anticancer agents and for elucidating the mechanisms of their activity. Upon treatment with compound S51, the MOLT-3 cells exhibited an increased rate of cell death at a volume of 100 µL. The compound demonstrated a 69.1% cell inhibition after 24 hours of incubation in fig 4.

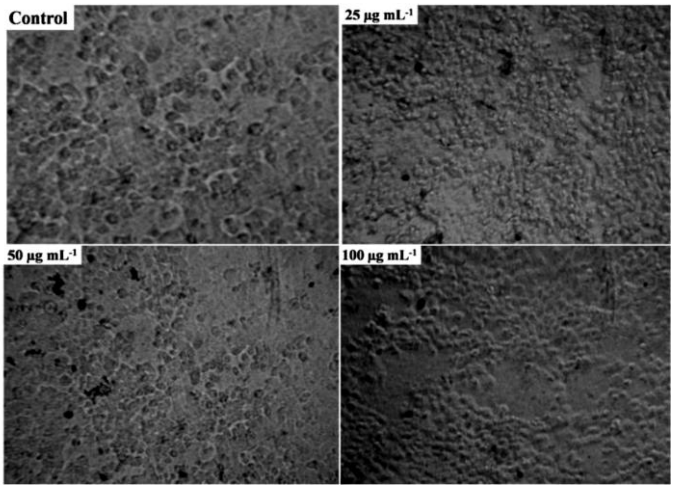

Figure 4 Cytotoxicity evaluation of g-C_3N_4/$ZnWO_4$ nanoparticles

 https://doi.org/10.5281/zenodo.13943054

5. CONCLUSION

In summary, we successfully synthesized exfoliated porous nanorods of metal-free g-C_3N_4 combined with $ZnWO_4$ metal nanocomposite using a cost-effective hydrothermal method. surface of the g-C_3N_4/$ZnWO_4$ nanocomposite. The findings from this work suggest a straightforward synthesis route for creating finely structured hybrid porous metal oxide nanocomposites, which can be effectively utilized in antimicrobial applications.

REFERENCE

1. Du, H, Chen, C, Krishnan, R, Krauss, TD, Harbold, JM, Wise, FW, Thomas, MG & Silcox, J 2002, 'Optical Properties of Colloidal PbSe Nanocrystals', Nano Letters, vol. 2, no. 11, pp. 1321-1324.
2. Dionne, GF & West, RG 1987, 'Magnetic and dielectric properties of the spinel ferrite system Ni0.65Zn0.35Fe2−xMnxO4', Journal of Applied Physics, vol. 61, no. 8, Sun, Z, Li, C, Du, X, Zheng, S & Wang, G 2018, 'Facile synthesis of two clay minerals supported graphitic carbon nitride composites as highly efficient visible-light driven photocatalysts', J. Colloid Interface Sci. vol. 511, pp. 268–276.
   pp. 3868- 3870.
3. Khin, MM, Nair, AS, Babu, VJ, Murugan, R & Ramakrishna, S 2012, 'A review on nanomaterials for environmental remediation', Energy Environ. Sci. vol. 5, pp. 8075-8109.
4. Bunaciu, EG & UdriŞTioiu, HY 2015, 'Aboul-Enein, X-ray diffraction: instrumentation and applications', Crit. Rev. Anal. Chem., vol. 45(4), pp. 289-299
5. Yang, Y, Zhang, C, Huang, D, Zeng, G, Huang, J, Lai, C, Zhou, C, Wang, W, Guo, H, Xue, W, Deng, R, Cheng, M & Xiong, W 2019, 'Boron nitride quantum dots decorated ultrathin porous g-C_3N_4: intensified exciton dissociation and charge transfer for promoting visible light-driven molecular oxygen activation', Appl. Catal. B vol. 245, pp. 87–99.
6. Shandilya, M, Rai, R & Singh, J 2016, 'Review: hydrothermal technology for smart materials', Adv. Appl. Ceram., vol. 115, pp. 354–376
7. Hurst, L. (2019). *Bacteriology*. Scientific e-Resources.

 https://doi.org/10.5281/zenodo.13943054

8. Sakoulas, G., & Moellering Jr, R. C. (2008). Increasing antibiotic resistance among methicillin-resistant Staphylococcus aureus strains. *Clinical infectious diseases*, *46*(Supplement_5), S360-S367.
9. Jaureguy, F., Landraud, L., Passet, V., Diancourt, L., Frapy, E., Guigon, G., ... & Brisse, S. (2008). Phylogenetic and genomic diversity of human bacteremic Escherichia coli strains. *BMC genomics*, *9*, 1-14.
10. Hamzah, A. A, Selvarajan, R. S, and Majlis, B. Y, 2017, 'Graphene for biomedical applications: A review', Sains Malaysiana, vol. 46, pp. 1125–1139.
11. Pant, B, Park, M, Lee, J, H, Kim, H, Y, and Park, S, J, 2017, 'Novel magnetically separable silver-iron oxide nanoparticles decorated graphitic carbon nitride nano-sheets: A multifunctional photocatalyst via one-step hydrothermal process', Journal of Colloid and Interface Science, vol. 496, pp. 343–352.
12. Xia, D, An, T, Li, G, Wang, W, Zhao, H, and Wong, P, K, 2016, 'Synergistic photocatalytic inactivation mechanisms of bacteria by graphene sheets grafted plasmonic AgAgX composite photocatalyst under visible light irradiation', Water Research, vol. 99, pp. 149–161.

 https://doi.org/10.5281/zenodo.13943054